e-Polymers **2006**, no. 051

http://www.e-polymers.org
ISSN 1618-7229

The influence of 4,4'-bis(6-hydroxyhexoxy)biphenyl moieties on properties of polyurethanes based on 4,4'-methylenebis(cyclohexyl isocyanate)

Tymon Łazarewicz,[1] * *Józef T. Haponiuk*,[2] *Adolf Balas*[3]

Polymer Technology Department, Gdańsk University of Technology, ul. Narutowicza 11/12 80-952 Gdańsk, Poland; Fax: (4858) 347-21-34. Email: [1]tymon@urethan.chem.pg.gda.pl; [2]jhp@urethan.chem.pg.gda.pl; [3]balas@chem.pg.gda.pl

(Received: 15 February, 2006; published: 14 August, 2006)

Abstract: Two series of polyurethanes (PUs) were synthesized from a low molecular weight diol – 4,4'-bis(6-hydroxyhexoxy)biphenyl (BH6), a high molecular weight diol – poly(1,6-hexylene adipate)diol (PHA) and 4,4'-methylenebis (cyclohexyl isocyanate) (HMDI) using two fractions of different trans,trans isomer content (u_T), respectively: 16%, 46%. The effect of low molecular diol content (u_B) in the total mass of the diols used for synthesis on properties of PUs was investigated by DSC, DTA, TGA, polarization microscopy, WAXS, DMTA and tensile testing. For segmented PUs microphase separation is observed and melting temperatures of hard segment (HS) microphases are almost constant within the series for $u_B \geq 40\%$. The growth of hard segment content (u_{HS}) induces rectilinear growth of crystallization enthalpy of HS microphases. PUs of $u_T = 46\%$ show birefringence of HS microphases at $u_B \geq 40\%$. Glass transition temperatures of HS microphases shift towards lower values with a decrease of u_B. PUs of $u_B = 80$ and 100% are stiff, for 20 - 60% elastomeric properties are observed, and in absence of low molecular diol moieties ($u_B = 0\%$) plastic behaviour is shown when stretched. Phase inversion is observed between $u_B = 60$ and 80%. Thermal stability of PUs (by TGA and DTA) does not depend on u_B and u_T.

Introduction

In recent years considerable attention has been paid on the structure – property relationships of polyurethanes (PUs) based on 4,4'-bis(ω-hydroxyalkoxy)biphenyls (BHn) [1-13]. Some PUs based on BHn are thermoplasts due to relatively low melting point of polymers in which macromolecules contain only short rigid mesogenic 4,4'-bis(oxy)biphenyl moieties. Both non segmented [1-7] and block [8-14] polymers have been described. Intensive work was focused on PUs based on tolylene 2,4-diisocyanate (TDI) [1-4, 8-11]. Penczek and co-workers investigated the influence of a 4,4'-bis(2-hydroxyethoxy)biphenyl (BH2) amount [8] and a high molecular diol length [9] on segmented PUs properties and microphase structure. PUs from BHn and other aromatic diisocyanates [3, 5, 6, 11-13] and aliphatic diisocyanates [2, 5, 11, 13, 14] were reported as well. Sun and Chang [13] described segmented PUs from 4,4'-bis(3-hydroxypropyloxy)biphenyl (BH3), poly(oxytetramethylene)glycol and 4,4'-methylenebis(cyclohexyl isocyanate) (HMDI). HMDI forms three geometrical isomers: trans,trans, cis,trans and cis,cis. Diisocyanate they used was a mixture of

geometrical isomers of unknown composition. We investigated PUs synthesised from 4,4'-bis(6-hydroxyhexyloxy)biphenyl (BH6), poly(1,6-hexylene adipate) (PHA) and HMDI fractions of determinated isomer distribution. We did not find any other reports concerning PUs from BH6 and HMDI together. The purpose of the paper is to present the effect of BH6 content (u_B) in the total mass of the diols used for synthesis on properties and structure of these PUs. Two series of PUs have been investigated – having 16 and 46% trans,trans isomer content of HMDI moieties (u_T). BH6 has been chosen as a chain extender due to rather long hexamethylene spacer separating mesogenic units from other rigid fragments in polymer chains. The increased length of spacers in BHn molecules strongly decreases phase transition temperatures of polymers [2, 3, 14].

Results and discussion

Properties of the chain extender

Liquid crystalline properties of BH6 have been investigated by DSC and polarization microscopy. DSC thermograms (Fig. 1) show two phase transitions during cooling (CR) and heating scans (T1) due to enantiotropic liquid crystalline behaviour.

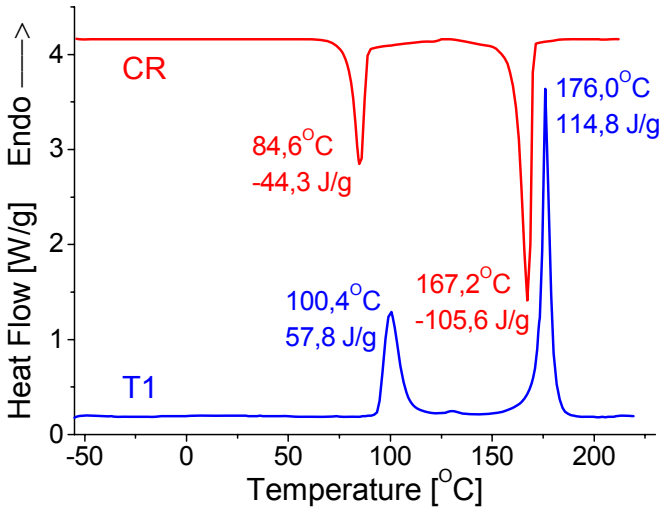

Fig. 1. DSC thermograms of BH6 (10°C/min).

The sample placed between slides was cooled from isotropic melt to temperature 172°C. The mosaic texture is observed (Fig. 2a) which is typical for smectic. The sample prepared by slow evaporating of p-dichlorobenzene from BH6 solution at 150°C displays mosaic texture with lancet-like shapes (Fig. 2b), typical for highly ordered modifications of smectic phase [21]. Inversion enthalpy is higher than melting enthalpy (twice) that seems to confirm smectic nature of the mesophase (Fig. 1).

Thermal stability of BH6 was characterised by TGA and DTA. The 5% weight loss temperature ($T_{5\%}$) is 400°C, the 10% weight loss temperature ($T_{10\%}$) is 420°C. DTA plots show endothermic peaks resulting from thermal decomposition at 425 and 440°C. The thermal stability of BH6 is high enough not to decompose during investigations of its liquid crystalline properties and for applied procedure of polyurethanes' synthesis. The thermal stability of PHA (the second diol monomer) is sufficient, too: $T_{5\%}$ = 360°C, $T_{10\%}$ = 380°C, endothermic peaks: 420°C, 565°C.

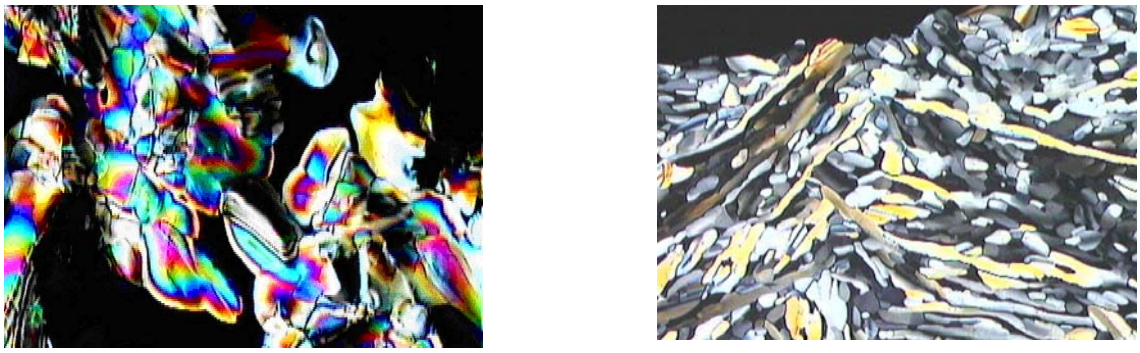

(a) (b)

Fig. 2. Mosaic textures of BH6: (a) 172°C, 42×; (b) 150°C, 28×.

The polyurethanes

The codes of PUs are Uu_B/u_T where u_B is BH6 content in the total mass of the diol monomers (BH6 + PHA) and u_T is trans,trans isomer content in HMDI that was used for the synthesis. Polymerization was carried out in the melt or concentrated p-dichlorobenzene solution in two steps. We synthesized non segmented U100/16, U100/46 from BH6, U0/16 from PHA and segmented terpolymers U80/16, U80/46, U60/16, U60/46, U40/16, U40/46, U20/16, U20/46 from two diol monomers – BH6 and PHA.

FTIR spectroscopy

Spectra of PUs of u_T = 16 and 46% are shown in Fig. 3 (a) and (b), respectively.

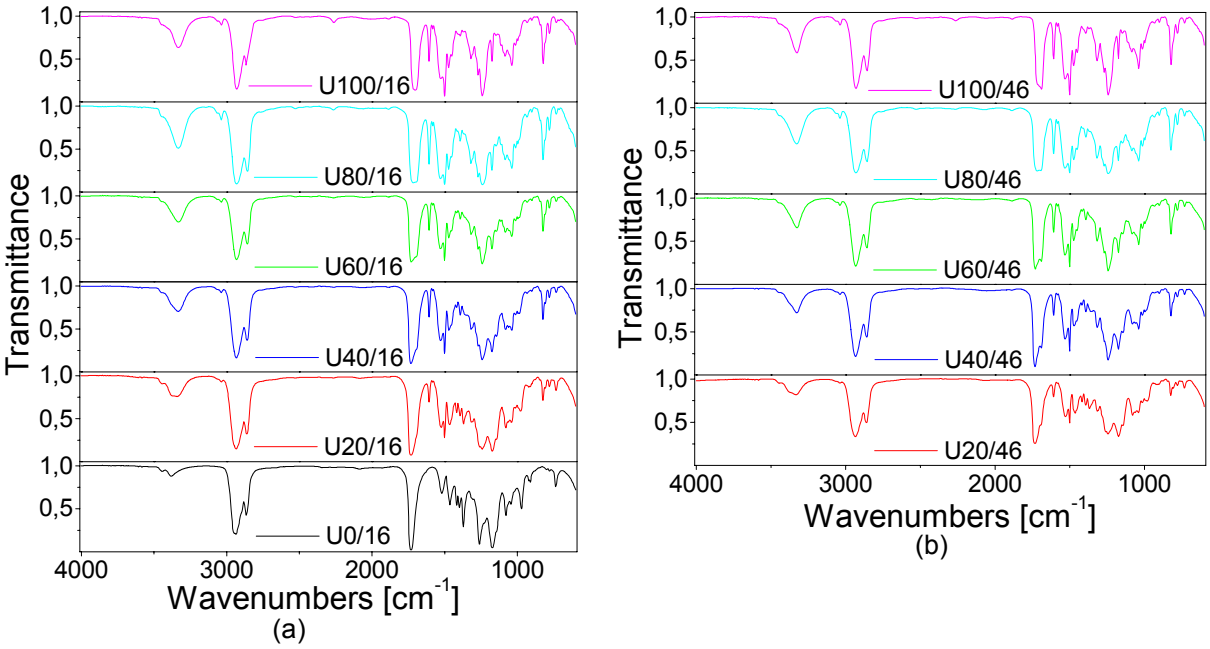

Fig. 3. FTIR spectra of the PUs (Uu_B/u_T) of (a) u_T = 16%, (b) u_T = 46%.

Structural characterization of the PUs measured by FTIR agrees with the prediction and indicates the following characteristic urethane group bands:

3323 - 3381 cm^{-1} s(wide)(ν, -**NH**-(CO)-O-); 1688 - 1705 cm^{-1} s(ν, -NH-(**C=O**)-O-) – I amide band; 1520 - 1537 cm^{-1} s(δ, -**NH**-(CO)-O-) – II amide band; 1393 - 1394 cm^{-1} w(ν, -O-(**C**=O)-**N**H-) – III amide band; 731 - 737 cm^{-1} w(γ, -**NH**-(CO)-O-).
Mesogenic unit (all PUs except for U0/16): 3061 - 3063 cm^{-1} w(ν, $\mathbf{C_{Ar}}$-**H**); 3036 - 3038 cm^{-1} w(ν, $\mathbf{C_{Ar}}$-**H**); 1884 - 1888 cm^{-1} w(**Ar**); 1607 cm^{-1} s(ν, **Ar**); 1501 cm^{-1} s(ν, **Ar**); 822 - 824 cm^{-1} s(γ, $\mathbf{C_{Ar}}$-**H**).
Ester group in soft segments (segmented PUs and U0/16): 1717 - 1734 cm^{-1} s(ν, C_{Alif}-(**C=O**)-O-).
Positions of urethane group bands of NH and C=O stretching vibrations depend on hydrogen bonding occurrence. Peaks s(ν, -**NH**-(CO)-O-) of non hydrogen bonded and hydrogen bonded urethane group for PUs are: 3420 - 3450 cm^{-1} and 3290 - 3330 cm^{-1}, respectively [22, 23]. Centred bands of PUs of u_B = 20 - 100% that we investigated are 3323 - 3339 cm^{-1} s(ν, -**NH**-(CO)-O-). These results show that most urethane groups are hydrogen bonded for the investigated PUs. For PUs of $u_B \geq 40\%$ with significant hard segment content (u_{HS}), hydrogen bonds between urethane groups are formed predominantly. For U0/16 the peak 3381 cm^{-1} s(ν, -**NH**-(CO)-O-) position is characteristic for relatively weak hydrogen bonds of urethane group formed between urethane and ester groups due to a high access of the latter. The broadened peak for PUs of u_B = 20% shows that both urethane – urethane and urethane – ester group hydrogen bond are formed. For segmented PUs of $u_B \geq 40\%$, the latter bands are not observed even though polymer chain contains ester groups. This seems to be due to microphase separation. The urethane groups are located mainly in the hard segment microphase, where concentration of ester groups from soft segments is low.

Thermal stability of the polyurethanes

Thermal stability of the PUs was investigated by TGA and DTA and the results do not depend on u_B and u_T. The temperatures $T_{5\%}$ = 355 - 365°C and $T_{10\%}$ = 370 - 380°C (heating rate 10°C/min) have been measured. DTA plots show endothermic peak resulted from thermal decomposition in range 400 - 430°C.

Differential scanning calorimetry

Block PUs (Uu_B/u_T) both of u_T = 16 and 46% demonstrate microphase separation and show phase transitions for hard segment (HS) and soft segment (SS) microphases separately, on heating run (Fig. 4, 5 and Tab. 1). The former occurs at higher, the latter at lower temperature.

Thermal behaviour of U100/16, U100/46 and the HS microphases of the block PUs. U100/16 and U100/46 shows glass transition (T_g) at about 78°C and 89°C (T3), respectively, followed by cold crystallization exotherm. The segmented PUs do not exhibit clear glass transitions of HS microphases in DSC thermograms.

U100/46 and U80/46 shows strongly thermal history dependent small endotherms (at different heating rates) that occur on thermograms of the first (T1) and the second heating run (T2) at temperature range 148 - 158°C (Fig. 6), not observed for u_T = 16% series. These peaks of low enthalpy could be related to formation of mesophases but polarization microscopy results do not confirm this conjecture. For T3 the endotherms are probably shifted to about 167°C (U100/46) and 163°C (U80/46) to form shoulders at inversion (transition to isotropic melt) peaks (Fig. 5).

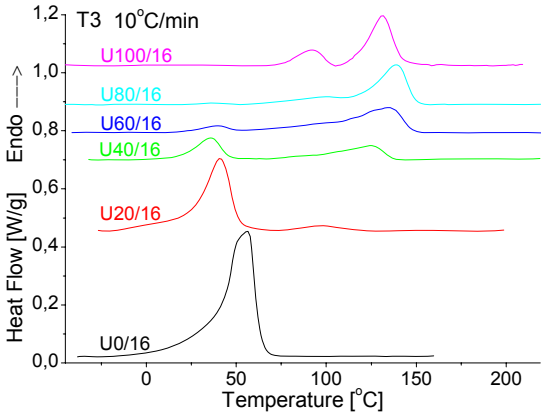

Fig. 4. DSC thermograms (the third heating run T3) of the PUs (Uu_B/u_T) of u_T = 16%.

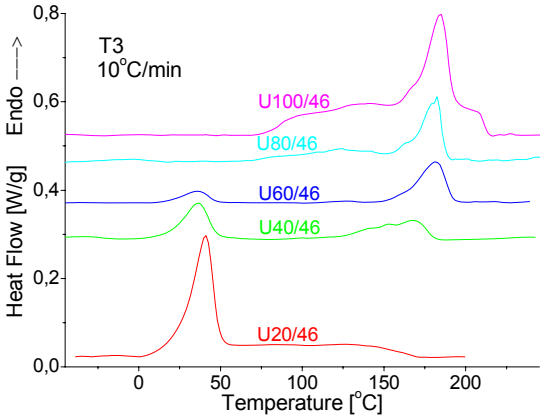

Fig. 5. DSC thermograms (T3) of the PUs (Uu_B/u_T) of u_T = 46%.

Tab. 1. Thermal transitions of hard segment (HS) and soft segment (SS) microphases (m) of the PUs (Uu_B/u_T).

Run	Peak	U100/16	U80/16	U60/16	U40/16	U20/16	U0/16	U100/46	U80/46	U60/46	U40/46	U20/46
Heating	T [°C]	132	139	134	126	98	-	184	182	183	167	144
(T3) HS m.	ΔH [J/g]	16	19	14	8.9	4.1	-	28	12	9.4	6.5	3.5
Cooling	T [°C]	91	95	89	80	53	-	124	121	121	108	84
HS m.	ΔH [J/g]	-20	-17	-13	-8.2	-1.8	-	-23	-18	-16	-10	-2.1
Heating	T [°C]	-	42	39	35	40	56	-	-	35	37	41
(T3) SS m.	ΔH [J/g]	-	~1	1.9	8.4	27	59	-	-	2.6	8.3	24

Melting point (T_M) of non segmented U100/16 is relatively low in comparison with PUs synthesised from BH6 and other diisocyanates, e.g. 2,4-TDI [1,2], 2,6-TDI [4], HDI [2], MDI [12]. In contrast, U100/46 forms an isotropic melt at relatively high temperature, namely 185°C (T3), due to higher u_T. For PUs of u_{HS} = 72 – 87%

(U80/16, U60/16, U80/46, U60/46), HS microphases melt at similar temperatures like U100/16 and U100/46, respectively, due to low miscibility of SSs within (Tab. 1). For U40/16 and U40/46 (u_{HS} = 54%) the endotherm is shifted towards lower values (Tab. 1) due to partial miscibility. For U20/16 and U20/46 (u_{HS} = 33%) only a very dim endotherm was observed. Enthalpies of the transition decrease with a decrease of u_{HS} but this dependence is not rectilinear.

PUs of u_{HS} = 100% and HS microphases of PUs of $u_{HS} \geq 55\%$ show exotherms of crystallization positioned at similar temperatures within the series of u_T = 16% and 46% (Fig. 7, Tab. 1). The dependence of crystallization enthalpy ΔH_{CR} on u_{HS} is rectilinear within the range 33 - 100% for cooling rate of 10°C/min (Fig. 8) and 20°C/min. No second exotherm is observed on cooling scans for U100/46 and U80/46, possibly due to delayed arranging time needed to form mesophase or crystalline phase in a viscous melt. Similar behaviour was described for PUs from BH2 [8].

Thermal behaviour of non segmented U0/16 and SS microphases of the block PUs both of u_T = 16% and 46%; the melting point of U0/16 at 56.5°C is close to that measured for PHA at 54.0°C (T3). SS microphase melting points of block PUs (U80/16, U60/16, U40/16, U20/16, U60/46, U40/46 and U20/16) are lower due to partial miscibility of HSs (Fig. 4, 5, Tab. 1). The crystallization exotherm peak of U20/46 is strongly decreased to -12°C in comparison with U0/16 (20°C). No crystallization endotherm of SS microphase is observed for other block PUs. Probably the rate of crystallization in a viscous melt of SS microphase is too low at applied cooling rates.

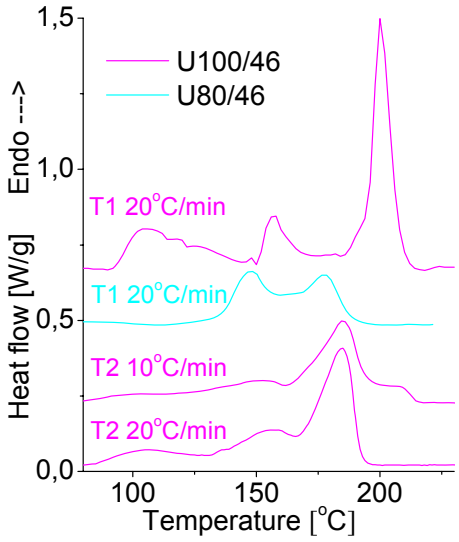

Fig. 6. DSC thermograms of U100/46 and U80/46 (Uu_B/u_T).

The melting and crystallization enthalpy of U0/16 ΔH_0 is about 60% of values measured for PHA. The moduli of melting enthalpies for segmented PUs decrease with a decrease of soft segment content u_{SS} (100 - u_{HS}) (Tab. 1) and are lower than quotient $|\Delta H_0| * u_{SS}$.

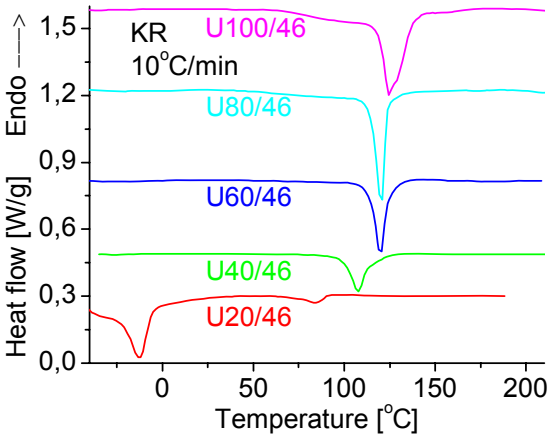

Fig. 7. DSC thermograms (the cooling run CR) of PUs (Uu_B/u_T) of u_T = 46%.

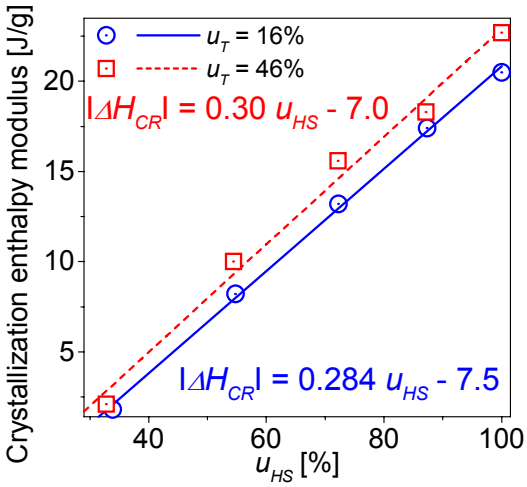

Fig. 8. The dependence of crystallization enthalpy on hard segment content (u_{HS}) for PUs of u_T = 16 and 46%.

Wide angle X - ray diffraction

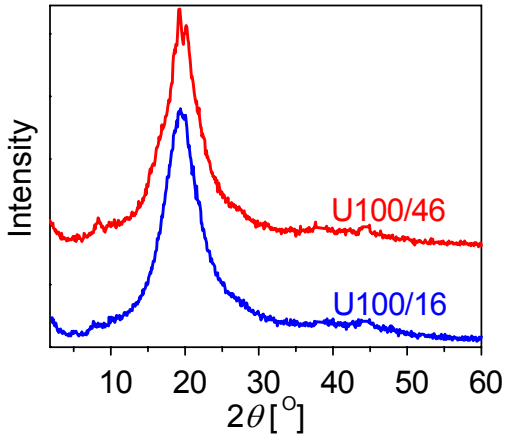

Fig. 9. WAXS spectra of PUs (Uu_B/u_T) U100/16 and U100/46.

Fig. 9 represents X-ray spectra for non segmented polymers U100/16 and U100/46, recorded at ambient temperature. For both PUs a wide diffraction maximum $2\theta = 19.75^{o}$ is observed that is related to parallel ordered fragments of macromolecules. Similar peaks at 20^{o} were observed for other PUs from BHn [2, 3, 11, 23, 24] and assigned to mesophase glass [23]. For U100/46 two sharp peaks overlap on the wide peak. This shows existence of crystalline regions.

Polarization microscopy

All PUs of $u_T = 46\%$ show birefringence at ambient temperature (e.g. Fig. 10a). At 65^{o}C PUs of $u_B = 40 - 100\%$ ($u_{HS} = 54 - 100\%$) are birefringent. Birefringence of U20/46 at 20^{o}C is due to SS microphase crystallinity only, because it is not observed at 65^{o}C, when SS microphase is melted. For U20/46 there is no birefringence of HS microphase, probably due to small size of crystalline regions within. The block PUs of $u_B = 40 - 80\%$ show birefringence of HS microphases that do not disappear when SS microphases are melted.

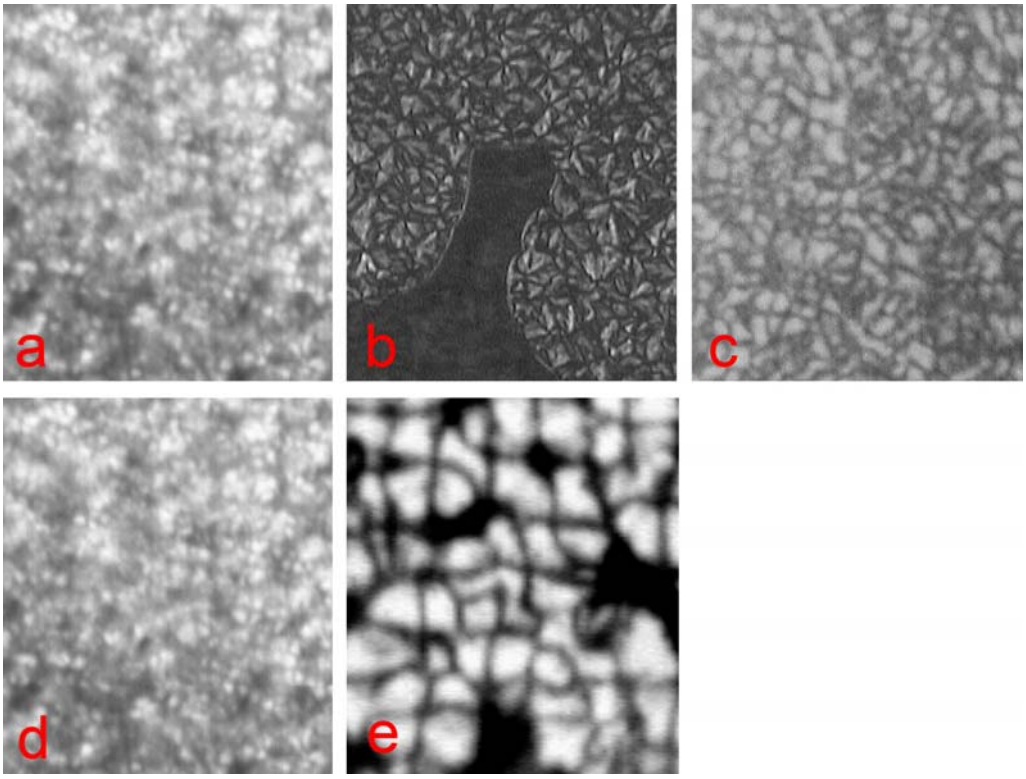

Fig. 10. Polarizing optical photomicrographs (Uu_B/u_T): a - U80/46 at 20^{o}C (500×); b - U100/46 at 170^{o}C (75×); c - U80/46 at 150^{o}C (500×); d - U40/46 at 150^{o}C (500×); e - U80/46 at 20^{o}C (500×).

PUs of $u_T = 16\%$ do not show birefringence for $u_B = 40 - 100\%$ regardless to temperature and thermal history. For U20/16 birefringence of SS microphase is observed at 20^{o}C and it disappears when heated to 65^{o}C. Similarly non segmented U0/16 shows birefringence at ambient temperature which is not observed for melted polymer at 65^{o}C. DSC results reported above (Tab. 4, 5) show that thermal properties of SS microphase do not depend on u_T that can be explained by gathering

of HMDI moieties outside of the SS microphases. The lack of birefringence of U40/16 suggests that birefringence of U40/46 is only due to HS microphase.

Textures of PUs of u_B = 40-100% and u_T = 46% (U100/46, U80/46, U40/46), obtained from slowly cooled melt (Fig. 10a-d) and formed by evaporating of the solvent from U80/46 solution at 150°C (Fig. 10e), exhibit the presence of spherulites, characteristic for crystalline phase. The results do not prove mesophase formation.

Dynamic mechanical thermal analysis

The characteristic temperatures evaluated from DMTA plots *logE''(T)* and *tgδ(T)* (Fig. 11a, 12a) are summarized in Tab. 2. PUs of high u_B show γ-relaxation probably due to methylene chains of BH6 moieties and β-relaxation peaks due to hydrogen bonded carbonyl of urethane groups are observed at about 30°C. Non segmented U0/16 shows a *logE''(T)* peak at -22°C and *E'(T)* starts to decrease at about -25°C (Fig. 11b) due to onset of glass transition. Glass transitions of SS microphases of the block PUs of u_{HS} = 33 and 55% from both of the series was observed at about -15°C (Fig. 11a, 12a). Glass transition temperatures of non segmented PUs: U100/16 and U100/46 are evaluated at 94 - 105°C by DMTA and agree with results obtained by DSC. The *E'* values decrease above 80 - 90°C (Fig. 11b, 12b). Block PUs U80/16 and U80/46 of u_{HS} = 87% show glass transition temperatures of HS microphases lower at about 20°C (Tab. 2). U0/16 and U20/16 shows the begining of the rapid growth of *tgδ(T)*, accompanied by decrease of *logE'(T)* above 50°C due to melting. The melting point of U100/46 is 157°C (*tgδ(T)*). Melting points of block PUs of u_{HS} = 54 and 72% are intermediate. The results discussed above obtained at frequency 1 Hz agree with that obtained at 0.1 Hz.

Tab. 2. Transition temperatures evaluated by DMTA.

Polymer (Uu_B/u_T)	Temperature [°C]							
	γ-Relaxation		T_g of SS m.	β-Relaxation	T_g of HS m.		Melting of	
							HS m.	SS m.
	logE''(T) Peak	*tgδ(T)* Peak	*logE''(T)* Peak	*logE''(T)* Peak	*logE''(T)* Peak	*tgδ(T)* Peak	*tgδ(T)* ↑↑	*tgδ(T)* ↑↑
U100/16	-48	-40	-	32	95	99	-	
U80/16	-50	-42	-	26	68	82	-	
U60/16	-41	-	-	19	-	70	-	
U40/16	-	-	-17	-	-	-	99	
U20/16	-	-	-15	-	-	-	-	49
U0/16	-	-	-22	-	-	-	-	53
U100/46	-55	-55	-	27	94	105	157	-
U80/46	-63	-63	-	-	80	90	-	-
U60/46	-	-	-11	-	-	78	123	-
U40/46	-	-	-21	-	-	-	90	-
U20/46	-	-	-2	-	-	-	-	-

HS m. – hard segment microphase; SS m. – soft segment microphase; ↑↑ - the begin of rapid growth.

DMTA results for block PUs show the microphase separation and dependence on u_{HS} partial miscibility of HSs and SSs. Dynamic mechanical properties observed for PUs of u_{HS} = 87% are similar to those of u_{HS} = 100%. This suggests that for U80/16 and U80/46 HSs form the continuous phases. DMTA results of block PUs of

$33 \leq u_{HS} \leq 54\%$ are close to that obtained for U0/16 that contains no hard segment. SSs of U60/16, U40/16, U20/16, U60/46, U40/46 and U20/46 form the continuous phases. Behaviour of the PUs of $u_{HS} = 72\%$ seems to arise from intermediate microphase structure close to phase inversion range of u_{HS}.

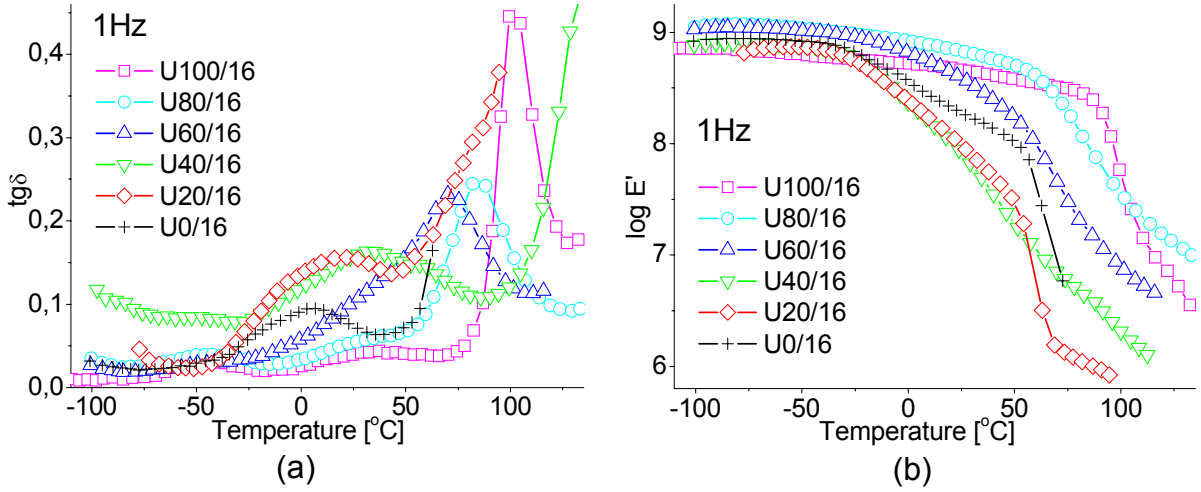

Fig. 11. The *tgδ(T)* (a) and *logE'(T)* (b) spectra of PUs (Uu_B/u_T) of u_T = 16%.

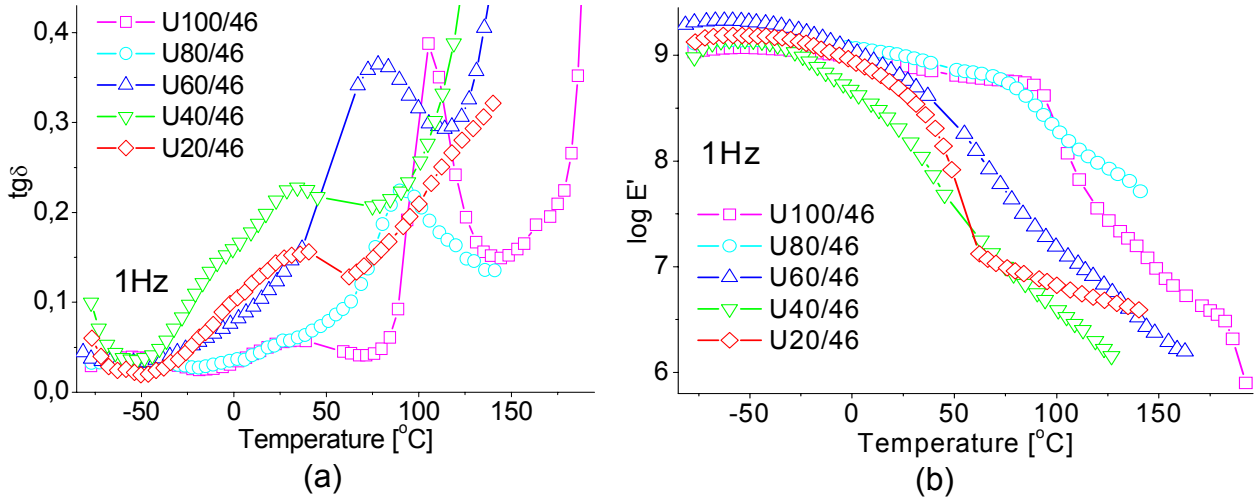

Fig. 12. The *tgδ(T)* (a) and *logE'(T)* (b) spectra of PUs (Uu_B/u_T) of u_T = 46%.

Mechanical properties

Stress-strain results are collected in Tab. 3. The highest ultimate tensile strength is shown by U100/16 and U80/16 but for U60/16 this is twice as low and similar to that measured for U40/16 and U20/16. The lowest ultimate tensile strength value is shown by U0/16. All block PUs of $u_T = 46\%$ show relatively high values of ultimate tensile strength in the range 33 - 31 MPa, however for non segmented U100/46 the ultimate tensile strength is lower. The PUs of $u_{HS} = 87$ and 100% are stiff but in the range 33 - 72% typical elastomeric properties are observed and ultimate elongations are from 300 to 630%. The best elastic properties are observed for $u_T = 46\%$ (U40/46, U20/46). The difference of elasticity between PUs of $u_{HS} = 72$ and 87% confirms the phase inversion occurrence. Non segmented polyurethane U0/16, as could be expected, shows no elastomeric behaviour. The highest ultimate elongation is accompanied by very high tension set that is about 80% of the former.

Tab. 3. Stress-strain results.

Property	Polyurethane (Uu_B/u_T)										
	U100/16	U80/16	U60/16	U40/16	U20/16	U0/16	U100/46	U80/46	U60/46	U40/46	U20/46
Ultimate tensile [MPa]	48	44	26	24	21	18	24	32	31	31	33
100% Modulus [MPa]	-	-	13	6.6	4.3	6.8	-	-	16	10	5.3
Ultimate elongation [%]	25	-	350	440	490	580	8	4	300	630	610
Tension set [%]	18	1	140	88	280	470	1	2	190	200	200

The Shore A hardness of the PUs is relatively high: 98 – 90°ShA for u_T = 16% and 99 - 93°ShA for u_T = 46%. In each polyurethane series the highest hardness is achieved for u_{HS} = 100% but the lowest for u_{HS} = 54%.

Conclusions

1. DSC, polarization microscopy DMTA and FT-IR studies reveal the microphase separation of the block PUs. Dynamic and static mechanical properties investigations show the phase inversion above u_{HS} = 72%.
2. The crystallization enthalpy is proportional to u_{HS} in the range u_{HS} = 33 - 100%.
3. Hard segment microphases of u_T = 46% shows birefringence for PUs of u_{HS} ≥ 54%. Birefringence of hard segment microphases is not observed at u_T = 16%. Soft segment microphases show birefringence for u_{HS} ≤ 33%.
4. Elastomeric properties are shown by PUs of u_{HS} = 33 - 72%. Better mechanical properties are achieved by elastomers of u_T = 46%.
5. The thermal stability of the PUs is not composition dependent.

Experimental part

Materials

6-Chloro-1-hexanol (Aldrich), cyclohexane (POCH), 4,4'-dihydroxybiphenyl (Aldrich), 1,4-dichlorobenzene (Koch-Light Laboratories LTD), DMF (POCH), ethanol anhydrous (POCH) was used as received.

Monomers

-BH6

BH6 was prepared by reaction of 37.2 g 4,4'-dihydroxybiphenyl (Aldrich) with 32.0 g NaOH followed by reaction of the phenolate with 120 g 6-chloro-1-hexanol (excess) in 300 cm^3 of anhydrous ethanol for 24 h under reflux. 6-Chloro-1-hexanol was added dropwise. BH6 was precipitated when reaction mixture was poured to cold water, then filtered off and washed with cold methanol. The precipitate was three times recrystallized from mixture of 140 cm^3 DMF and 470 cm^3 ethanol and finally recrystallized from 1-butanol. After every recrystallization step product was washed with methanol. The precipitate was then dried at 110°C in vacuum to the constant mass. Yield: 59.1 g (76.5%). Elementary analysis results: Cl – not detected; C: 74.76%; H: 9.12%; (calculated: C: 74.58%; H: 8.87%). The structure was confirmed by ^{1}H-NMR and FT-IR.

^{1}H NMR ($CDCl_3$) 200 MHz a: 7.47(d, 4H); b: 6.96(d, 4H); c: 3.98(t, 4H); d: 3.66(t, 4H); e: 1.82(qui, 4H); f: 1.58(qui, 4H); g: 1.6 - 1.4(m, 8H); h: 1.49(s, 2H) – disappears after D_2O treatment. (Scheme 1)

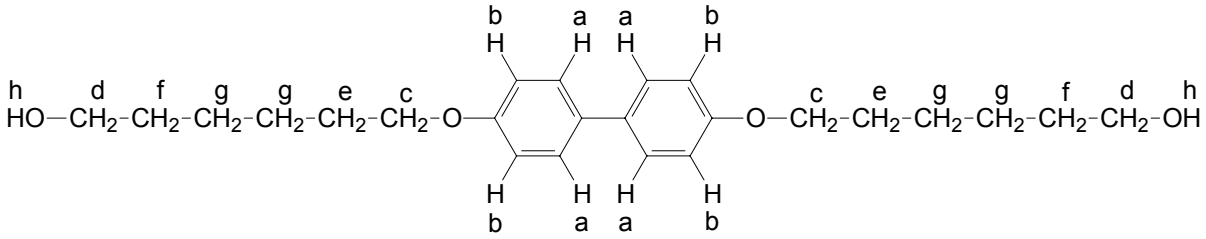

Scheme 1. Hydrogen atom codes for ^{1}H NMR results for BH6.

-PHA

PHA of molecular weight 3000, hydroxyl number 37.9 mg KOH/g (Poles H-3, manufactured by Zakłady Chemiczne Zachem S.A.) was dried at 130°C in vacuum.

-HMDI

HMDI (Aldrich) was distilled in vacuum (150 - 152°C, 5 mmHg) and then used for synthesis of the first series of PUs. Isomer distribution was as follows: 15.8% trans,trans-, 52.2% cis,trans-, 31.9% cis,cis-HMDI. NCO group concentration was 32.8 ±0.8%. Fraction of isomer distribution: 45.8% trans,trans-, 34.8% cis,trans-, 19.4% cis,cis-HMDI was used for synthesis of the second series of PUs. HMDI fractions enriched in the trans,trans-isomer were separated by crystallization. The diisocyanate was rectified (150 - 152°C, 5 mmHg) before crystallization. The first crystallization was carried out from melt at 0°C, the second – from melt at 20°C and the third – from cyclohexane solution at 20°C, according to the procedure described in [15]. The obtained solid and liquid fractions were distilled in vacuum. Isomer distributions were determined by gas chromatography. Fraction of 46% trans,trans isomer content was prepared by mixing fractions.

Polyurethane synthesis

Polyaddition was carried out in two steps under dry N_2. The PUs were synthesised according to two procedures. Synthesis in the melt was performed for PUs from HMDI of trans,trans isomer content (u_T) 16% and one polyurethane of u_T = 46% – U20/46 (Tab. 4). Synthesis in the solution was necessary for the most PUs of u_T = 46% due to high melting points of prepolymers and forming polymers.

-Polyurethane synthesis carried out in the melt

In the first step (3 h, 155 – 165 °C) an excess of HMDI reacted with diol reagents to give a prepolymer of about 3% NCO content. Then NCO content was determined (see below). In the second step (3 h, 170 - 180°C) the prepolymer was reacted with a calculated extra amount of diol, so that the [NCO]/[OH] molar ratio at the 2nd step was 1.05.

-Polyurethane synthesis carried out in the solution

This method was used for PUs of u_T = 46% at u_B = 40 - 100% (Tab. 5). Polyaddition was carried out in two steps under reflux under dry N_2 atmosphere. In the first step (3 h) an excess of HMDI reacted with diol reagents to give a prepolymer of about 3%

NCO content. p-Dichlorobenzene (10 - 20 g) was used as a solvent. Temperature of oil bath was from 150°C at the beginning to 180°C at the end of reaction. The NCO content of prepolymer solution was then determined (see below). In the second step (3 h, 170 - 180°C) the prepolymer was reacted with calculated extra amount of diol, so that the [NCO]/[OH] molar ratio at the 2nd step was 1.05. Polymer solution was placed in Teflon Petri dish and covered. p-Dichlorobenzene was slowly evaporated (150°C) to form a plate. Then the plate was heated at 170 - 180°C in vacuum (6 - 10 mmHg) for about 5 h to remove the rest of the solvent.

Tab. 4. Polyurethane syntheses carried out in the melt.

Polyurethane (Uu_B/u_T)		U100/16	U80/16	U60/16	U40/16	U20/46	U20/16	U0/16
The 1st stage	HMDI [g]	6.18	5.48	4.64	3.71	2.60	2.60	1.22
	BH6 [g]	7.24	5.91	4.46	2.76	0.70	0.70	-
	PHA [g]	-	1.91	4.14	6.78	9.93	9.93	6.14
Concentration of NCO in prepolymer [%]		2.93	3.12	2.94	2.91	2.70	3.10	2.71
Number-average molecular weight of prepolymers		2870	2690	2860	2890	3110	2710	3100
The 2nd stage	Prepolymer [g]	11.24	10.91	11.35	11.50	11.44	11.45	5.61
	BH6 [g]	1.44	1.49	1.46	1.49	1.34	1.55	-
	PHA [g]	-	-	-	-	-	-	5.10
Yield [g]		12.69	12.40	12.81	12.99	12.79	13.00	10.71
Hard segment content u_{HS} [%]		100	87.3	72.3	54.7	32.8	33.9	-

Tab. 5. Polyurethane syntheses carried out in the p-dichlorobenzene solution.

Polyurethane (Uu_B/u_T)		U100/46	U80/46	U60/46	U40/46
The 1st stage	HMDI [g]	6.18	5.43	4.64	3.71
	BH6 [g]	7.24	5.91	4.46	2.75
	PHA [g]	-	1.92	4.14	6.78
Concentration of NCO [%] (measured)	Prepolymer solution	1.23	1.13	1st stage in melt	1.66
	Prepolymer	3.03	2.88	2.87	2.83
Number-average molecular weight of prepolymers		2770	2920	2930	2970
The 2nd stage	Prepolymer solution [g]	28.40	30.06	-	19.40
	Prepolymer [g]	11.50	11.83	10.69	11.37
	BH6 [g]	1.53	1.49	1.34	1.41
Yield [g]		12.88	13.29	11.72	12.71
Hard segment content u_{HS} [%]		100	87.2	72.2	54.4

-Determination of NCO group concentration in sample

A typical titrimetric NCO group determination was performed. Prepolymer (~0.4 g) or its p-dichlorobenzene solution (0.6 - 1 g) was placed in chlorobenzene containing 0.5×10^{-3} mol dibutylamine and heated under reflux to dissolve. Then 50 cm^3 acetone and Bromophenol Blue were added and titrated with 0.05 mol/dm^3 HCl (solution in water) till a yellow colour. Blank determination results were used to calculate NCO concentration.

Elementary analysis results for selected PUs are given in Tab. 6.

Tab. 6. Elementary analysis results.

Polyurethane ($U u_B/u_T$)	Observed [%]			Calculated [%]		
	C	H	N	C	H	N
U100/16	71.59	9.07	4.39	72.17	8.70	4.36
U80/16	70.47	9.11	3.86	70.98	8.73	3.87
U60/46	68.96	9.19	3.34	69.54	8.76	3.32
U40/16	67.50	9.17	2.62	67.90	8.80	2.64
U20/16	65.71	9.32	1.82	65.93	8.85	1.84
U0/16	63.21	9.18	0.85	63.54	8.91	0.93

p-Dichlorobenzene has been used as a solvent due to its extremely low hygroscopicity, the lack of reactivity to isocyanates, high dissolving power to PUs at elevated temperatures and high thermal stability. p-Dichlorobenzene, the solvent of relatively high boiling point (174.1°C, 760 mmHg), seems to be a good choice for PUs from cycloaliphatic diisocyanates which need higher temperatures to react with diols due to lower reactivity [16]. The obtained PUs are of higher thermal stability in comparison with PUs synthesized from aromatic diisocyanates [17]. The use of o-dichlorobenzene as a solvent for synthesis of low molecular compounds – diisocyanates was reported [18,19] but we did not find any other report about the use of any isomer of dichlorobenzene for a polyurethane synthesis.

Polyurethane U0/16 was synthesized from PHA and HMDI as a model polymer to compare properties of SS microphases of block polymers with. The value $u_{HS} = 0$ is assigned (Table 1) because single cycloaliphatic diisocyanate moieties between polyadipate moieties are not assumed as HS.

Measurements

Elementary analysis was performed on a Carlo Erba Instruments Elementary Analyser EA 1108.

^{1}H-NMR was carried out in $CDCl_3$ on a Varian Gemini 200 MHz instrument.

FTIR investigations of polymer film (~10 μm) were performed on an IFS 66 & FRA 106 Brukner spectrometer.

Gas chromatography was carried out on a Fisons GC 8000 instrument equipped with column – RTX5 300 mm × 0.25 mm, 5% biphenyl + 95% poly(dimethylsiloxane). A NPD detector was used.

TGA and DTA thermograms were recorded using a MOM Budapest Derivatograph OD104. Investigations were carried out under N_2 atmosphere, at a heating rate of 10°C/min. The sample weight was 200 - 300 mg.

DSC investigations were performed on a Perkin Elmer DSC7 differential scanning calorimeter under N_2 purge gas, at a scanning rate of 10°C/min (samples ~15 mg): samples were heated from -60°C to 160-260°C (T1), then quenched at maximal rate; heated from -60°C to 150-250°C (T2); cooled to -60°C (CR) and heated to 160 - 260°C (T3). The calorimeter was calibrated with pure indium and water. The raw data were processed with graphic software using baseline correction. WAXS investigations were carried out on a Seifert URD6 diffractometer with CuK_α radiation, equipped with Anton-Paar Kratky camera at ambient temperature. The angle 2θ range was 1 - 60° and the step was 1°.

Polarization microscopy observations were performed with crossed polarizers on a MIN-8 and a PZO microscope. A Mettler Toledo thermal analyser with Hot Stage HP92 was used. Two BH6 samples were observed. The first one was prepared as a melt between glass slides. The second was prepared by slow evaporating of p-dichlorobenzene from BH6 solution placed at a glass slide at 150°C. Three types of polymer samples were prepared: a) A 0.2 mm film prepared by evaporating p-dichlorobenzene from polymer solution placed on a Teflon Petri dish at 150°C, slowly cooled and then stored about 3 month at ambient temperature prior to use. b) A polymer thin film melted between two glass slides, then slowly cooled (0.1°C/min) to temperature equal to that applied during observations and maintained at this temperature several hours prior to observations. c) Prepared by slow evaporating of p-dichlorobenzene from the polyurethane solution placed at a glass slide at temperature range of mesophase to be expected.

DMTA investigations were carried out on a Polymer Laboratories DMTA PL MK III Standard apparatus, using the bending mode at frequency of 1 Hz. Data were collected from -80 to 130 - 190°C at a heating rate of 4°C/min.

Stress – strain measurements were performed on a VEB Rauenstein FPZ 100 tensile testing machine at speed of 100 mm/min at ambient temperature.

Hardness was tested with the use of a VEB Rauenstein Shore A tester at ambient temperature.

Acknowledgements

This work was supported by State Committee for Scientific Research (Grant No. 014045). We are grateful to Dr M. Wiergowski (Gdańsk University of Technology) for determination by gas chromatography the isomer distribution of HMDI fractions.

References

1. Stenhouse, P. J.; Valles, E. M.; Kantor, S. W.; MacKnight W. J.; *Macromolecules* **1989**, 22, 1467.
2. Hsu, T. F.; Lee, Y. D.; *Polymer* **1999**, 40, 577.
3. Lee, J. B.; Kato, T.; Yoshida, T.; Uryu, T.; *Macromolecules* **1993**, 26, 4989.
4. Papadimitrakopoulos, F.; Hsu, S. L.; MacKnight, W. J.; *Macromolecules* **1992**, 25, 4671.
5. Lin, C. K.; Kuo, J. F.; Chen, C. Y.; *Eur. Polym. J.* **2000**, 36, 1183.
6. Valentova, H.; Sedlakova, Z.; Nedbal, J.; Ilavsky M.; *Eur. Polym. J.* **2001**, 37, 1511.
7. Sato, M.; Komatsu, F.; Takeno, N.; Mukaida, K.; *Makromol. Chem. Rapid. Commun.* **1991**, 12, 167.
8. Penczek, P.; Frish, K. C.; Szczepaniak, B.; Rudnik, E.; *J. Polym. Sci. Polym. Chem. Part A: Polym. Chem.* **1993**, 31, 1211.

9. Szczepaniak, B.; Frish, K. C.; Penczek, P.; Mejsner, J.; Leszczyńska, I.; Rudnik, E.; *J. Polym. Sci. Part A: Polym. Chem.* **1993**, 31, 3223.
10. Tang, W.; Farris, R. J.; MacKnight, W. J.; Eisenbach, C. D.; *Macromolecules* **1994**, 27, 2814.
11. He, X.; Jia, X.; Yu, X.; *J. Appl. Polym. Sci.* **1994**, 54, 207.
12. Mix, R.; Gähde, J.; Goering, H.; Schulz, G.; *J. Polym. Sci. Part A.: Polym. Chem.* **1995**, 33, 1523.
13. Sun, S. J.; Chang, T. C.; *J. Polym. Sci. Part A: Polym. Chem.* **1996**, 34, 771.
14. Haponiuk, J. T.; Strankowski, M.; Łazarewicz, T.; *J. Thermal. Anal. Cal.* **2003**, 74, 609.
15. Seneker, S. D.; Born, L.; Schmelzer, H. G.; Eisenbach, C. D.; Fisher, K.; *Colloid. Polym. Sci.* **1992**, 270, 543.
16. Couvret, D.; Brosse, J. C.; Chevalier, S.; Senet, J. P.; *Eur. Polym. J.* **1991**, 27, 193.
17. Fabris, F.; in *Advances in Urethane Science and Technology*, vol. 4. red. Frish, K. C.; Reegen, S. L.; Westport: Technomic Publishing Co.; **1976**, p. 89.
18. von Siefken, W.; *Ann.* **1949**, 562, 6.
19. Mormann, W.; Brahm, M.; *Polymer* **1993**, 34, 187.
20. Khan, N.; Patel, V. L.; Bashir, Z.; Price, D. M.; *J. Polym. Sci. Part. B: Polym. Physics* **1995**, 33, 1957.
21. Dehmus, D.; Richter, L.; *Textures of Liquid Crystals*. Weinheim, New York: Verlag Chemie, 1978.
22. Papadimitrakopoulos, F.; Sawa, E.; MacKnight, W. J.; *Macromolecules* **992**, 25, 4682.
23. Brunette, C. M.; Hsu, S. L.; MacKnight, W. J.; *Macromolecules* **1982**, 15, 71.
24. Smyth, G.; Valles, E. M.; Pollack, S. K.; Grebowicz, J.; Stenhouse, P. J.; Hsu, S. L.; MacKnight, W. J.; *Macromolecules* **1990**, 23, 3389.